Electronic structure of the transparent *p*-type semiconductor (LaO)CuS

Shin-ichiro Inoue, Kazushige Ueda, and Hideo Hosono
Materials and Structures Laboratory, Tokyo Institute of Technology, 4259 Nagatsuta, Midori, Yokohama 226-8503, Japan

Noriaki Hamada
Department of Physics, Faculty of Science and Technology, Science University of Tokyo, 2641 Yamazaki, Noda 278-8510, Japan
(Received 25 May 2001; published 6 December 2001)

(LaO)CuS with a layered structure is a transparent *p*-type semiconductor (band gap = 3.1 eV), which gives an excitonic absorption/emission near the band edge even at room temperature. We examined the electronic structure of this material by photoemission and inverse photoemission spectroscopy and considered the nature of the electronic structure by comparing the photoemission spectra with the band structure calculated by the full-potential linearized augmented plane-wave method within the local-density approximation. It was proved that the top of the valence band is primarily composed of well-hybridized states of Cu $3d$ and S $3p$ states, while the bottom of the conduction band consists mainly of Cu $4s$ states. The band gap of (LaO)CuS was found to be a direct-allowed transition type through the analysis of the symmetry of these states. It was also found that the dispersion of the valence band is relatively large due to the considerable hybridization of Cu $3d$ and S $3p$ states. This dispersed valence band is responsible for the emergence of *p*-type electrical conduction in this material. On the other hand, the dispersion of the conduction band is rather small, probably because of the layered structure, in comparison with typical *n*-type conducting materials. This small dispersion of the conduction band leads to the wide band gap and high stability of excitons in (LaO)CuS.

DOI: 10.1103/PhysRevB.64.245211 PACS number(s): 71.20.Nr, 79.60.Bm, 71.15.Mb, 72.10.−d

I. INTRODUCTION

The recent development of optoelectronic devices such as short-wavelength light-emitting and laser diodes shows that wide and direct-band-gap materials are of importance technologically.[1–6] Fabrication of transparent p-n junctions is essential for the development of semiconductor devices based on these materials. However, most transparent conductive materials are *n*-type conductors, and moreover, the conversion of these materials to *p*-type conductors is generally difficult because of the strong monopolarity. Therefore, much effort has been made for a long time to find transparent *p*-type conducting materials.[7–10]

Recently, we examined electrical transport and optical properties of (LaO)CuS finding the following characteristics.[11] (i) This material is transparent in the visible region (band gap is ~3.1 eV). (ii) The electrical conduction is *p* type and the conductivity is largely increased by substitution of Sr^{2+} ions for La^{3+} ions. (iii) The sharp absorption and emission peaks originating from excitons are distinctly seen near the absorption band edge even at room temperature.[12] From these findings, (LaO)CuS is considered to be an attractive candidate material for optoelectronic devices in ultraviolet and/or blue regions.

Figure 1 shows the crystal structure of the layered oxysulfide (LaO)CuS.[13–15] The symmetry and space group are tetragonal and $P4/nmm$, respectively, and there are two formula units in the unit cell. (LaO)CuS has a two-dimensional structure composed of alternately stacking Cu_2S_2 layers, which consist of edge-sharing CuS_4 tetrahedra and La_2O_2 layers along the [0 0 1] direction. In most oxides containing monovalent Cu^{1+}, the Cu^{1+} ions usually form O-Cu-O dumbbell structures. On the other hand, Cu^{1+} ions in sulfides prefer to take tetrahedral coordination. In (LaO)CuS, Cu^{1+} ions take tetrahedral coordination because the Cu^{1+} ions are located in the sulfide layers.

Although the crystal structure of (LaO)CuS was determined definitely, its electronic structure, which is indispensable for understanding the unique optoelectric properties of this material, has not been investigated yet. Therefore, we performed experimental and theoretical investigation concerning the electronic structure of this material. In this paper, we report the electronic structure (occupied and unoccupied states) of (LaO)CuS examined by normal/inverse photoemission spectroscopy and first-principles energy-band calculations.

II. EXPERIMENT

A. Sample preparation

An Sr-doped (5 at %) specimen was used for photoemission measurements to avoid charging. Polycrystalline Sr-

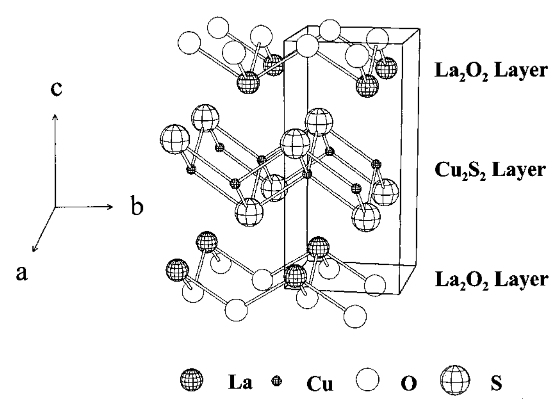

FIG. 1. Crystal structure of (LaO)CuS. Note that each layer in the unit cell has a +2 or −2 charge.

doped (LaO)CuS was prepared by solid-state reaction using La_2O_3, La_2S_3, Cu_2S, SrS, and S powders in appropriate proportions. The mixed reactant was pelletized and sealed in an evacuated silica tube, and heated at 1073 K for 6 h. After regrinding and pelletizing by a cold isostatic press at 800 $kg\,cm^{-2}$, the pellet was heated at 1173 K for 6 h. The crystalline phases of the sample were identified by powder x-ray diffraction (Rigaku Rint 2500), and each diffraction peak was indexed as arising from (LaO)CuS.

B. Photoemission and inverse photoemission measurements

Photoemission spectroscopy (PES) and inverse photoemission spectroscopy (PES) measurements were carried out at room temperature using a home-built instrument.[16] The PES spectra were measured by using several excitation sources. In the ultraviolet photoemission spectroscopy (UPS) measurement, He I (21.2 eV) and He II (40.8 eV) resonance radiations from a He discharge lamp VG Microtech UVL-HI were used, and the energy resolution was better than 120 meV. In the x-ray photoemission spectroscopy measurement, Mg $K\alpha$ (1253.6 eV) radiation was used, and the energy resolution was ~1.4 eV. The IPES spectra were measured in a bremsstrahlung isochromat spectroscopy (BIS) mode. The BIS spectra were obtained by detection of photons of 9.5 eV using a band-pass-type photon detector. The energy resolution of the BIS spectra was ~0.5 eV. The base pressure was 1×10^{-7} in the PES chamber or 5×10^{-8} Pa in the IPES chamber. The sample surface was scraped *in situ* with a diamond file just before each measurement in order to obtain clean and fresh surfaces.

C. First-principles band calculations

The first-principles band calculations that we performed are based on density-functional theory within the local-density approximation (LDA).[17,18] An analytical form of the exchange-correlation potential proposed by Vosko, Wilk, and Nusair was used in the calculations.[19] The Kohn-Sham equations were self-consistently solved by applying the full-potential linearized augmented plane-wave (FLAPW) method.[20] The FLAPW calculation for (LaO)CuS was carried out under the reported crystal structure: the space group of $P4/nmm$, and the lattice constants of $a=b=3.999$, $c=8.53$ Å.[14] The coordination axes of *x*, *y*, and *z* in the calculation were set to the lattice axes of *a*, *b*, and *c*, respectively. The muffin-tin (MT) radii were set to 2.7 (1.43) for La, 2.1 (1.11) for Cu, 1.9 (1.01) for S, and 1.4 a.u. (0.743 Å) for O. Inside the MT spheres, the angular momentum expansion was truncated at $l_{max}=7$ for the potential and 6 for the wave function. The wave functions outside the MT spheres were expanded in terms of plane waves up to a cutoff energy of 10 Ry. Self-consistent calculations were carried out with 45 meshed **k** points in the irreducible wedge of the Brillouin zone. The calculation was iterated until the calculated total energy of the crystal converges into less than 0.01 mRy. A tetrahedron method was used to obtain the total and partial densities of states. The total density of states (DOS) was evaluated by referring to the energy eigenvalues for all states, while the partial DOS was done for the states within the MT spheres. It should be noted that more than 70% of the total DOS is in the MT sphere in the occupied states, while more than 60% of the total DOS is out of the MT sphere in the unoccupied states in this calculation.

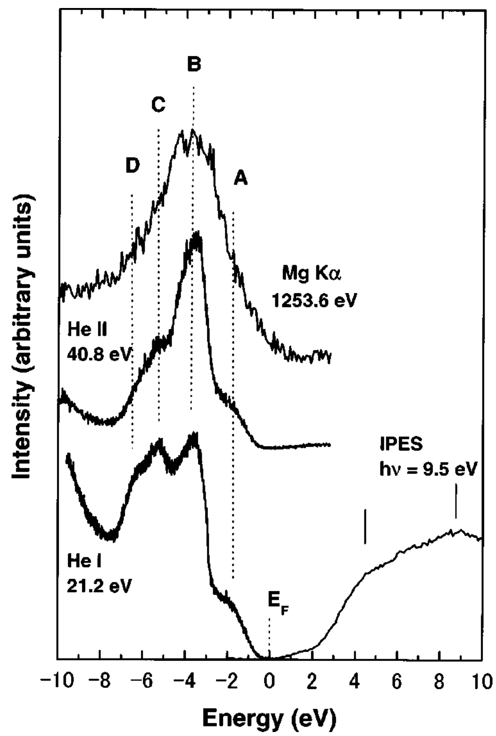

FIG. 2. PES and IPES spectra of (LaO)CuS. Photon energies of 21.2, 40.8, and 1253.6 eV were used in the PES measurements, and that of 9.5 eV was detected in the IPES measurement. Fermi energies of the PES or IPES spectra were set to zero in the energy scale.

III. RESULTS

A. Photoemission and inverse photoemission spectra

Figure 2 shows the PES spectra ($E_{ex}=21.2$, 40.8, and 1253.6 eV) and IPES spectrum ($h\nu=9.5$ eV) of (LaO)CuS. The PES and IPES spectra were shown by setting each Fermi energy to zero in the energy scale. The band gap estimated from band edges in these spectra is ~3 eV, which is consistent with the optical band gap obtained from the optical transmission measurement on the thin film.[11] The IPES spectrum shows two broad peaks at 4–5 and 8–9 eV. The PES spectra show four distinct bands peaking at about −1.9, −3.6, −5.3, and −6.3 eV, and these peaks are indexed as A to D. The intensity of the most intense peak B at −3.6 eV increases with increasing photon energy. The photoionization cross section of the Cu 3*d* states rapidly increases with an increase in the photon energy from 21.2 (He I) to 1252.6 eV (Mg $K\alpha$) in comparison with the cross section of S 3*p* or O 2*p* states.[21] Therefore, it is reasonable to interpret that the peak B in the PES spectra arises primarily from the Cu 3*d* states. The intensities of the other peaks A, C, and D in the PES spectra decrease with increasing photon energy. These peaks are suggested to be anion *p* states or hybridized states taking into account the energy levels of orbitals of the component ions.

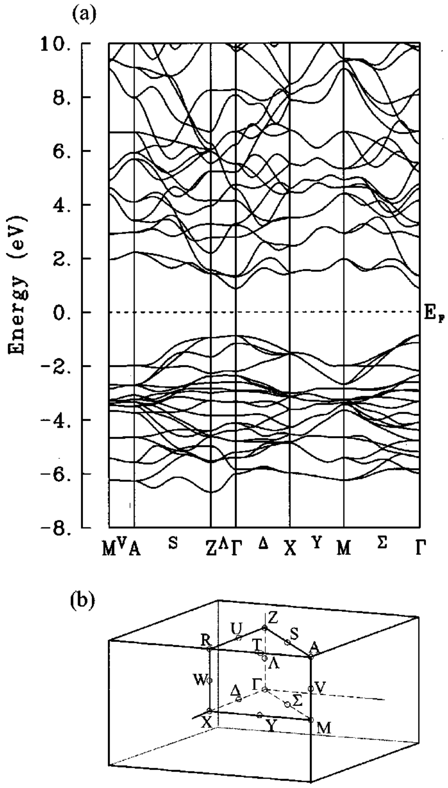

FIG. 3. Calculated band structure of (LaO)CuS along the high-symmetry lines in the first Brillouin zone. The position of the Fermi energy is indicated by a dashed line at 0 eV.

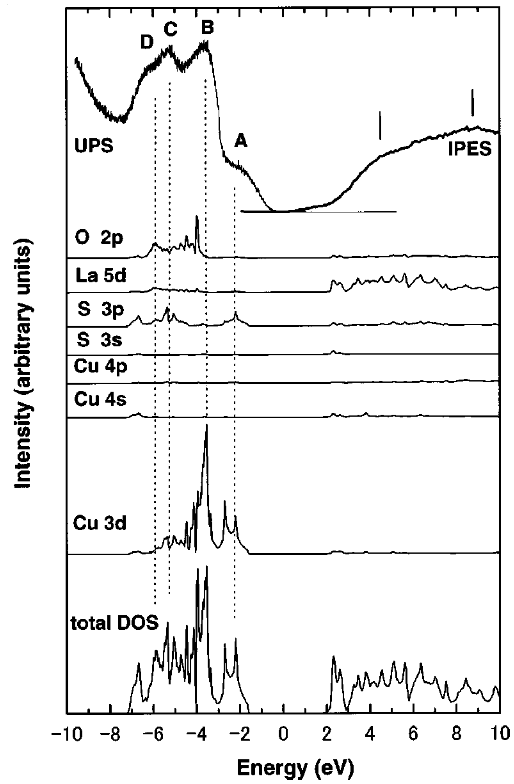

FIG. 4. Electronic structure of (LaO)CuS near the Fermi energy region: the total and partial densities of states along with UPS (He I) and BIS spectra.

B. Energy-band calculations

Figure 3(a) shows the energy-band structure of (LaO)CuS calculated by the FLAPW method along the high-symmetry **k** lines [see Fig. 3 (b)]. It is found from the figure that both the valence-band maximum (VBM) and the conduction-band minimum (CBM) are located at the Γ point ($\mathbf{k}=0$), indicating that (LaO)CuS is a direct-gap semiconductor. The direct band gap is calculated to be 1.75 eV, which is smaller than the value (~3.1 eV) experimentally determined by optical transmission and photoemission measurements. This discrepancy (underestimation) is commonly seen for band-gap estimation under LDA.

The effective masses of electrons (m_c^*) and holes (m_h^*) were estimated from the curvature near the CBM and VBM at the Γ point. The results are $m_c^*=0.29$, $m_h^*=2.8\,\mathrm{m}$ for a heavy hole, 0.34 m for a light hole in the *x* or *y* direction, and $m_c^*=0.36$, $m_h^*=1.2\,\mathrm{m}$ in the *z* direction.

The analysis of symmetry without considering the spin-orbital interaction revealed that the wave functions at VBM, which degenerate twofold, are labeled Γ_5', and have symmetry similar to *x* and *y*. The wave function at CBM is labeled Γ_1, and has symmetry like z^2. The polarization vectors $\mathbf{E}\perp c$ and $\mathbf{E}\| c$ in the tetragonal lattice (D_{4h}) belong to Γ_5' and Γ_2', respectively. The direct products of the irreducible representations between the polarization vectors and the wave function of the valence band are given as

$$\Gamma_5'\times\Gamma_5'=\Gamma_1+\Gamma_2+\Gamma_3+\Gamma_4, \tag{1a}$$

$$\Gamma_2'\times\Gamma_5'=\Gamma_5 \tag{1b}$$

The direct product $\Gamma_5'\times\Gamma_5'$ contains the representation of Γ_1, which is the same as the wave function of the conduction band. This means that the optical transition between the VBM and CBM is allowed for $\mathbf{E}\perp c$. Although anisotropic electrical and optical properties are expected in (LaO)CuS, to the best of our knowledge, there are no experimental data showing the anisotropic properties because only the polycrystalline specimen is available at the present stage.

IV. DISCUSSION

A. Comparison of total and partial densities of states with photoemission spectra

Figure 4 shows the total and partial densities of states of (LaO)CuS obtained by the FLAPW band calculations along with UPS (HeI) and IPES spectra. The band gap of the calculated DOS was enlarged so as to meet the experimental value (~3.1 eV). The experimental and theoretical curves were compared on the same energy scale referred to the Fermi energy.

In the occupied states, the feature of the calculated total DOS, which consists mainly of Cu $3d$, S $3p$, and O $2p$ states, is in good agreement with the PES spectra, the experimentally observed DOS. The ratio of theoretical photoemission cross sections of the Cu $3d$, S $3p$, and O $2p$ states at $h\nu=21.2\,\mathrm{eV}$ is about 1.0: 0.6: 1.4.[21] The values of each cross section of these states are roughly comparable. Therefore, the calculated DOS can be compared with the photoemission spectrum without correction of the cross section in a first approximation. The main peak B at about -3.6 eV in the PES spectra is assigned to the maximum at -4 eV in the total DOS. The bands responsible for the maximum originate from well-localized Cu 3d states. Since S 3p states are hardly seen in the energy region of peak B, this intense structure of B indicates a nonbonding character. This assignment for peak B is basically consistent with the tentative assignment based on the photon energy dependence of the PES spectra. The band C peaking at about -5.3 eV predominantly consists of S 3p states arising from bonding interaction between Cu 3d and S 3p states. The peak D at about -6.3 eV consists of O 2p (major) and La 5d (minor) states. The band of the total DOS in the energy range between about -1.5 and -3 eV corresponds to the experimentally observed shoulder marked as A at about -1.9 eV. This structure originates from well-hybridized Cu 3d and S 3p states.

In the unoccupied states, two broad structures are observed at around 4–5 and 8–9 eV in the IPES spectrum. These two bands cannot be resolved clearly in the calculated partial DOS. In addition, the intensity of the partial DOS in these energy regions is small because the most densities of states (about more than 60% of the total DOS) in the unoccupied states are out of the MT spheres. However, we tentatively consider that the structure around 4–5 eV is due to La 5d states with a slight admixture of Cu 4s states, and the structure around 8–9 eV consists mainly of La 5d and Cu 4p states.

B. Features arising from the band structure near the band gap

We first focus on the band structure in the vicinity of the VBM. According to the calculations, the upper valence band is primary composed of well-hybridized states between Cu 3d and S 3p states, and has a relatively large band dispersion as compared with typical oxide semiconductors like SnO_2.[22] This upper valence band of (LaO)CuS was clearly observed as a broad shoulder A in the PES spectra. This broad feature of the upper valence band results from the considerable hybridizations, that is, the large overlaps between Cu 3d and S 3p wave functions in the Cu_2S_2 layers. Moreover, the large overlaps between these wave functions basically stem from the close atomic energy levels of Cu 3d and S 3p orbitals, indicating the strong covalent character of CuS bonds in the Cu_2S_2 layers or at the upper valence bands. Therefore, it is reasonable to expect that the large dispersion near the VBM, especially along the Δ and Σ lines, results in the small effective mass of hole carriers and causes p-type electrical conduction in (LaO)CuS.

Next discussed is the electronic structure around the CBM. The lowest conduction band is considered to consist mainly of Cu 4s states, although the Cu 4s states cannot be clearly seen in the partial DOS, and no remarkable structure originating from a Cu 4s band was resolved in the IPES spectrum. However, this consideration is supported by the result that the band around the CBM is almost isotropic in any direction, for example, the Γ-X, Γ-M, and Γ-Z directions, indicating its s-like character. As seen in the band diagram of Fig. 3(a), the dispersion of this band is relatively small for s states in comparison with typical n-type transparent conducting oxides such as ZnO.[23] This implies that Cu 4s orbitals in (LaO)CuS are not spread as widely as Zn 4s orbitals in ZnO. As a result, this small dispersion leads to the wide band gap of about 3.1 eV in spite of the large dispersion of the top of the valence band, which is large enough to provide transparency in the visible region. Furthermore, the small dispersion around the CBM gives a relatively large effective mass of electrons, which will explain the high stability or the large binding energy of excitons in (LaO)CuS as discussed in a previous paper.[12]

V. SUMMARY

The present study examined the electronic structure of a transparent p-type semiconductor (LaO)CuS by both photoemission spectroscopy and first-principles band calculations. The results obtained are summarized as follows:

(i) Both the valence-band maximum and the conduction-band minimum are located at the Γ point ($\mathbf{k}=0$), and the direct transition between these two states is allowed for $\mathbf{E}\perp c$.

(ii) The upper valence band, which is primarily composed of the well-hybridized states between Cu 3d and S 3p states, has a large dispersion in the x or y direction, which is expected to cause strong anisotropic hole transport properties.

(iii) The lowest conduction band mainly composed of Cu 4s states has a relatively small band dispersion in comparison with typical n-type conducting oxides. This small dispersion leads to the wide band gap of this material and a relatively large effective mass of electrons.

[1] M. A. Hasse, J. Qui, J. M. DePuydt, and H. Cheng, Appl. Phys. Lett. **59**, 1272 (1991).

[2] D. M. Bagnall, Y. F. Chen, Z. Zhu, T. Yao, S. Koyama, M. Y. Shen, and T. Goto, Appl. Phys. Lett. **70**, 2230 (1997).

[3] P. Yu, Z. K. Tang, G. K. L. Wong, M. Kawasaki, A. Ohtomo, H. Koinuma, and Y. Segawa, J. Cryst. Growth **184/185**, 601 (1998).

[4] S. Nakamura, M. Senoh, N. Iwasa, and S. Nagahama, Appl. Phys. Lett. **67**, 1868 (1995).

[5] S. Nakamura, M. Senoh, S. Nagahama, N. Iwasa, T. Yamada, T. Matsushita, Y. Sugimoto, and H. Kiyoku, Appl. Phys. Lett. **70**, 1417 (1997).

[6] H. Ohta, K. Kawamura, M. Orita, N. Sarukuta, M. Hirano, and H. Hosono, Appl. Phys. Lett. **77**, 475 (2000).

[7] H. Kawazoe, M. Yasukawa, H. Hyodo, M. Kurita, H. Yanagi, and H. Hosono, Nature (London) **389**, 939 (1997).

[8] H. Yanagi, S. Inoue, K. Ueda, H. Kawazoe, and H. Hosono, J. Appl. Phys. **88**, 4159 (2000).

[9] A. Kudo, H. Yanagi, H. Hosono, and H. Kawazoe, Appl. Phys. Lett. **73**, 220 (1998).
[10] M. Joseph, H. Tabata, and T. Kawai, Jpn. J. Appl. Phys., Part 2 **38**, L166 (1999).
[11] K. Ueda, S. Inoue, S. Hirose, H. Kawazoe, and H. Hosono, Appl. Phys. Lett. **77**, 2701 (2000).
[12] K. Ueda, S. Inoue, N. Sarukura, M. Hirano, and H. Hosono, Appl. Phys. Lett. **78**, 2333 (2001).
[13] M. Palazzi, C. Carcaly, and J. Flahaut, J. Solid State Chem. **35**, 150 (1980).
[14] M. Palazzi, C R. Acad. Sci. III **292**, 789 (1981).
[15] K. Ishikawa, S. Kinoshita, Y. Suzuki, S. Matsuura, T. Nakanishi, M. Aizawa, and Y. Suzuki, J. Electrochem. Soc. **138**, 1166 (1991).
[16] H. Yanagi, Ph.D. thesis, Tokyo Institute of Technology, 2001.
[17] P. Hohenberg and W. Kohn, Phys. Rev. **136**, B864 (1964).
[18] W. Kohn and L. J. Sham, Phys. Rev. A **140**, 1133 (1965).
[19] S. H. Vosko, L. Wilk, and M. Nusair, Can. J. Phys. **58**, 1200 (1980).
[20] E. Wimmer, H. Krakauer, M. Weinert, and A. J. Freeman, Phys. Rev. B **24**, 864 (1981).
[21] *Atomic Calculation of Photoionization Cross-Sections and Asymmetry Parameters*, edited by J.-J. Yen (Gordon and Breach, New York, 1993).
[22] J. Robertson, J. Phys. C **12**, 4767 (1979).
[23] P. Schroer, P. Kruger, and J. Pollmann, Phys. Rev. B **47**, 6971 (1993).